Available online at www.sciencedirect.com
SCIENCE DIRECT®
Journal of Nuclear Materials 337–339 (2005) 286–290
journal of nuclear materials
www.elsevier.com/locate/jnucmat

Spectroscopic measurements of plasma flow in the SOL in C-Mod

K. Marr *, B. Lipschultz, B. LaBombard, J.L. Terry

MIT Plasma Science and Fusion Center, 167 Albany Street #216, Cambridge, MA 02139, USA

Abstract

We evaluate the limits of the spectroscopic measurement of scrape-off layer flows utilizing HeII excitation emission (486.6 nm) in the inboard, high-field, scrape-off region. Velocities are inferred from the Doppler shift of the HeII emission line for lower and upper single-null discharges, exhibiting differences of up to 20 km/s between the two. Unfortunately at high temperatures (>30 eV), the short ionization time, compared to momentum transfer times, makes the interpretation difficult for those plasma regimes. The inferred variations of plasma flows near the inner wall correlates with Langmuir Mach probe measurements in its dependence on magnetic topology. However the flow magnitudes are different. The discrepancy between probe and spectroscopic measurements is likely due a combination of two effects: the magnitude of gas injection needed to achieve a reasonable signal is found to be too perturbative and loss of high-energy He ions from the viewing volume.

PACS: 52.25.−b; 52.25.Rv; 52.25.Vy; 52.30.−q
Keywords: Alcator C-Mod; Edge plasma; Helium; Plasma flow; Spectroscopy

1. Introduction

Plasma flows are the focus of intense scrutiny in tokamak devices. To understand the mechanism(s) that drives these flows and how they might affect plasma performance, we must be able to measure accurately the flows in both the core and the scrape-off layer (SOL). Plasma flows and flow shear are likely related to the local electric field and affect the core confinement by affecting the pedestal parameters. Recent results from C-Mod [1,2] indicate that SOL flows may be coupling to the core and thus affecting the power threshold for transition to H-mode. These flows also play a role in impurity transport in the SOL; many experiments have documented flow of C to the inner divertor and the build-up of C layers and trapping of H/D/T there [3].

Gas plume measurements have established that at the inboard midplane SOL in Alcator C-Mod, the plasma flow is primarily along the field [4]. Measurements of flow velocities using charge-exchange recombination spectroscopy (CXRS) and an energetic neutral beam are fairly standard but restricted to the outside half of tokamak plasmas (see for example, Ref. [5]).

Here we attempt to provide an independent examination of the flow along field lines in the inboard SOL region by making spatially localized measurements of Doppler shifted HeII Paschen-α line (3–4) emission.

* Corresponding author. Tel.: +1 781 316 2668; fax: +1 617 253 0627.
E-mail address: kmarr@mit.edu (K. Marr).

0022-3115/$ - see front matter © 2004 Elsevier B.V. All rights reserved.
doi:10.1016/j.jnucmat.2004.10.029

Field has obtained poloidal velocities using line-integral measurements of the HeII, BIV, and CIII lines [6]. Doppler measurements of parallel flow, localized by a gas-puff, of D_α [7] and HeII line [8] have been made previously on C-Mod. However, measurement limitations were not fully addressed. Simpler than the standard CXRS technique, our method can be used for inboard measurements. The measurements are made by puffing neutral helium from a local nozzle and then recording the excitation emission. The Doppler shift of the emitted line leads directly to a measurement of the velocity of the emitting He^+ projected along the line-of-sight. The temperature of the emitting ions can also be computed through the thermal broadening of the emission spectra.

The flow measurements are from a variety of L-mode and H-mode, deuterium discharges for a range in plasma densities. Most discharges included RF heating.

2. Experiment setup and analysis method

The scrape-off layer in the Alcator C-MOD tokamak is defined as those magnetic field surfaces outside of the separatrix (last closed flux surface). An in-vessel telescope and fiber optic array are employed to observe the inboard midplane of the SOL. Six fibers view parallel to the local magnetic field through the inboard SOL (see Fig. 1). The chord spot size of each individual fiber is 3.75 mm with tangency points on the inner SOL separated ~4 mm in major radius. A top–down view of the region of interest is shown in Fig. 1.

He gas is puffed from a tube embedded in the inner wall and oriented with its axis normal to the wall, i.e. perpendicular to the viewing chords. This 'crossed-beam' geometry localizes the emission toroidally and obviates the need for any spatial inversion of signals to obtain a radial profile [9]. The location of the gas puff tube is also shown in Fig. 1. For this experiment, neutral helium was injected, but alternate gases will be discussed below for use in future work.

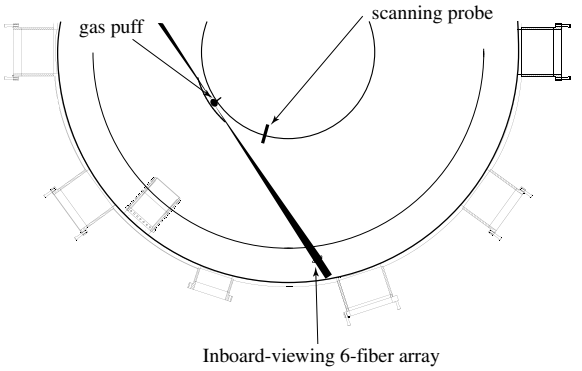

Fig. 1. Diagram showing the location of the Inboard SOL viewing array. Also shown are the locations of the gas puff and scanning probe.

A Chromex *f*/4, 0.25 m, Czerny–Turner, 3-grating spectrometer was used to disperse the emission spectra across a 1242 pixel (in wavelength) × 16 input CCD. The 1200 line/mm grating, used for this study, provides a range of ~70 nm on the CCD. Typically, the camera was read out every 58 ms. Such a short focal length spectrometer is not optimized for Doppler velocity measurements but was used in this work to decide if further efforts were warranted. Doppler T_i measurements were obtained from the fits but imprecise instrumental functions rendered them very uncertain and they are not the subject of this paper. A Zinc calibration lamp was utilized to provide reference lines (nearest at 468.014 nm) for wavelength calibration, dispersion, and the instrumental line shape. During the discharges one of the sixteen spectrograph inputs (or 'views') was dedicated to the Zinc lamp thus providing constant reference lines and wavelength calibration for that view (and therefore for all views using a relative view-to-view wavelength calibration). We also checked the relative calibration of the various views by comparing inferred velocities when all views were inside the separatrix, their viewing location varying with respect to the separatrix both during a discharge and from discharge to discharge.

The helium line at 468.475 nm was chosen because it is one of the strongest lines in the range we can measure. Because the viewing chords are nearly parallel to the magnetic field, the emission spectrum is Zeeman split primarily into two equal components (σ) flanking the $B = 0$ emission wavelength. Emissions from the outer-wall portions of the viewing chord and the fact that the view is not perfectly parallel to the magnetic field result in a small central component (π) at the emission wavelength completing the familiar Zeeman triplet. It has been shown that the Zeeman splitting can be fairly well approximated by a simple relation dependent only upon the strength of the magnetic field [10]. For helium the splitting is given by $\Delta = \alpha B$ (nm) where Δ is the wavelength difference between the peaks of the two σ components, $\alpha = 0.0205206$ nm/T and B is the local magnetic field. (Generally $B = 5.3$ T on axis; $R_{axis} = 67.0$ cm.) We fit the emission spectra with an instrumental function convolved with a Gaussian for each of the Zeeman triplet components. During the fit, these three components are then allowed to shift as a whole (retaining the splitting defined above) and simultaneously broaden to mimic the Doppler effects due to heating and bulk flow. The height of the central component is allowed to change with respect to the side components. We have classified fits with the central peak intensity at 10–20% of its possible maximum (twice as tall as the side components when viewed perpendicularly to B) as 'good' fits.

3. Experimental results

A useful way to classify the data collected is by the shape of the plasma magnetic equilibrium flux surfaces. Three types of plasma magnetic equilibria were utilized: lower single-, double-, and upper single-nulls (LSN, DN, and USN respectively). The last closed flux surface or separatrix will be designated the 'primary' separatrix. Its corresponding dominant x-point is closest to the lower (upper) divertor for LSN (USN) plasmas. Further out in the SOL there is a secondary separatrix with an x-point near the opposite divertor. For a double-null equilibrium the two x-points are essentially on the same flux surface, the primary separatrix, one near each divertor. The distance between the separatrices associated with the upper and lower x-points, measured at the outer midplane, is the definition of ssep (another name used is drsep). Due to uncertainty in the magnetic equilibrium analysis we define a range for DN discharges of $|\text{ssep}| < 3$ mm. Thus an LSN (USN) discharge has an ssep less (greater) than this range. All three configurations have $B \times \nabla B$ pointing towards the lower divertor for these experiments.

We now consider three discharges to illustrate the effect of the magnetic topology on the measured flows. We have selected one discharge for each null configuration, all similar in density to reduce the number of variables. Fig. 2 presents an overview of the effect of magnetic topology on parallel velocity. The data is taken from a view close to the inner wall and outside the separatrix. Certain features should be noted. Lower single-null data shows the most positive velocities. Positive in this sense is defined as co-current, which is clockwise when viewed from above. As ssep is increased into the double-null regime, we can see a rapid shift towards faster velocities. The upper single-null data falls in the middle of the range of velocities experienced by the double null sweep. (The double-null data was obtained by varying ssep during a single shot.) The total range covered by the velocities is approximately −5 km/s to −35 km/s.

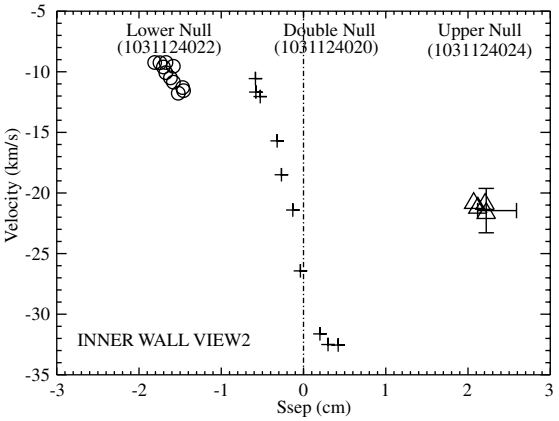

Fig. 2. Typical effect of changing ssep on the velocity for three discharges. Varying the distance between the two separatrices (ssep) causes significant differences in the measured velocity.

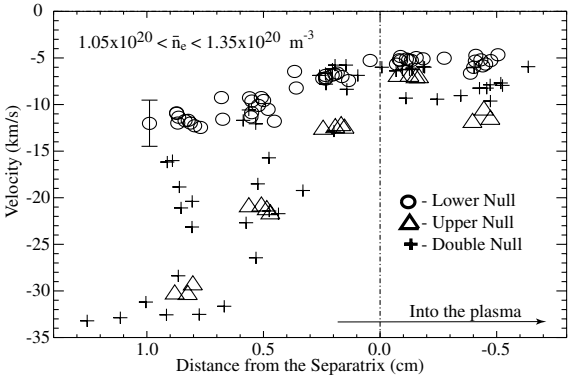

Fig. 3. Velocity vs. distance from the separatrix for the discharges of Fig. 2.

Fig. 3 shows an inboard SOL velocity profile using five of the six inboard views. (The sixth view signal was too low.) Again it is seen that the lower single-null data (circles) have the most positive velocity for any radial position. None of the data is positive, the relevance of which, with respect to other measurements, will be discussed below. Error bars of at least 2 km/s are estimated for the data.

We have compared velocities inferred with and without RF, and during L- and H-modes. There do not appear to be significant differences among them leaving magnetic topology as the dominant factor. At the transition from L- to H-mode we do observe a temporary (~50 ms) drop in SOL flow velocities near the wall of up to 5 km/s.

4. Modeling the emission spectra

Because we are injecting gas into the plasma the thermal and momentum equilibration times and the ionization time are key parameters. If the injected atoms are ionized too quickly they will not have time to equilibrate to the background plasma before emitting. The bulk velocity inferred from this situation would therefore be different from the background plasma velocity.

We are able to characterize the ionization and equilibration times by using the following thermal and momentum exchange rates, ν_{th} and ν_{momentum} [11,12], and the ionization rate, ν_{ion}.

$$\nu_{\text{th}} \cong 1.95 \times 10^{-12} \frac{n_1 Z_1^2 Z_2^2 \mu_1^{1/2}}{T^{3/2} \mu_2} = 6.9 \times 10^{-13} \frac{n(m^{-3})}{(T(eV))^{3/2}} s^{-1}$$

$$\nu_{\text{momentum}} \cong \frac{3}{4} \nu_{\text{th}}, \quad \nu_{\text{ion}} = n(m^{-3}) S_{\text{ion}}(T_e), \tag{1}$$

where subscript 1 indicates the background ions and 2 the impurity 'test particles', n and T the background plasma density and temperature ($T_i = T_e$ assumed), ln $\Lambda = 14$ has been used, Z is the charge number, μ is the atomic mass, and S_{ion} is the He^+ ionization rate [13]. The approximation that the test particle is colder and more massive than the background ions ($T_2/\mu_2 \ll T_1/\mu_1$) is used to arrive at the limit expressed by Eq. (1). The momentum equilibration rate does not have the same scaling as for thermalization but it can be approximated as shown for this plasma parameter range.

A comparison of equilibration times can be found in Table 1. The temperatures and densities used are roughly matched to that found in the SOL using the inner wall scanning probe [2]. Acknowledging uncertainties in the rates and conditions (e.g. T_i is probably 2–3T_e), it is still clear that above ~30 eV the measured He ion velocity will deviate from that of the background plasma. Though not obvious from the table, it should be noted that the ratio in the last column is essentially density independent. This table indicates that inside the separatrix ($T_e > 60$ eV) the measured velocity should be small compared to the background plasma flow and fairly independent of position. This is consistent with measurements as typified by what is found in Fig. 3.

To investigate the effect of the equilibration on the emission line shape and shift we have created a crude model to simulate the line emission from a group of room-temperature test ions at zero bulk velocity that have been injected into a fixed n_e and T_e plasma. This ignores any equilibration occurring in the neutral state via ion–neutral collisions. We modeled 'packets' of He^+ ions as they equilibrated with the background plasma. Two simultaneous processes were followed: the number of He^+ ions was reduced exponentially with time constant τ_{ion} and, secondly, the energy (directed velocity) of the remaining ions was increased, approaching that of the background plasma with time constant τ_{thermal} (τ_{mom}) assuming $T_i = T_e$. This process is stepped forward in time until all test particles in the packet are ionized. Emission occurs with each step and an emission lineshape is generated. Generally, the emission has an asymmetric line shape dependent on the fraction of the population that does not equilibrate to the background flow. Simple Gaussian fits of the line shape underestimate the flow velocity (and temperature) by 30–40% for n_e and T_e values typical of the separatrix region dropping to a small error farther out (e.g. below 30 eV). The analysis of the lineshape inside the separatrix has proven to be too uncertain for the purposes of inferring flow.

Table 1
Calculation of the local equilibration and ionization rates based on measured background plasma conditions

Density (10^{20} m^{-3})	Temperature (eV)	ν_{momentum} (s^{-1})	ν_{ion} (s^{-1})	$\tau_{\text{momentum}}/\tau_{\text{ion}}$
1.0	50	1.4×10^5	1.1×10^5	0.79
0.75	40	1.5×10^5	6.0×10^4	0.40
0.5	30	1.5×10^5	2.3×10^4	0.15
0.3	20	1.7×10^5	4.8×10^3	0.03
0.25	10	4.0×10^5	2.0×10^2	<0.01

$\tau_{\text{mom}} = 1/\nu_{\text{mom}}$, $\tau_{\text{ion}} = 1/\nu_{\text{ion}}$.

It was also a concern that the particles might flow out of the viewing chord as they equilibrate with the background. Though not as much of an issue at the bulk velocity, some ions will attain higher thermal velocities that take them out of the viewing area much faster. A 50 eV He ion would traverse an ~10 cm distance (overlap of flux tube with viewing chord) in a few microseconds leaving behind lower energy ions leading to a distorted measured lineshape. A full Monte-Carlo model would be required to assess these issues properly.

5. Discussion

Our results are inconsistent in magnitude with other measurements on C-Mod. Previous work in which visible emission of a locally produced carbon plume was imaged has shown that the plume direction (longitudinal) reverses from lower to upper single-null shots [4]. Similarly, measurements made using a reciprocating Langmuir (Mach) probe that measures plasma flow upstream and downstream have shown that lower single-null shots generally have a positive (co-current) rotation. This probe measures a change in velocities between lower and upper single-null shots of over 80 km/s [1].

Our data does not display the same direction reversal evidenced by the above diagnostics. The range in Mach probe velocity data is ~4 times that of the HeII Doppler data. Even considering the reduced velocities predicted by the model for high-temperature situations, we cannot explain this difference. Our HeII measurements generally follow the relative trends shown by the Mach probe indicating that use of this method as a relative velocity measurement may be reasonable. Certainly it has the advantage over probes of being able to measure velocity profiles for the entire discharge.

We believe that there are at least two potential reasons for the above discrepancies between the HeII Doppler measurements and the other velocity measurements. First, as discussed above, the ions leave the viewing region as they thermalize, leaving behind the less equilibrated ions. The second possibility is that the gas puff is perturbative. Solving a simple steady-state approximation for the injection rate's, Γ_{in}, relationship to local He density ($\Gamma_{\text{in}} = n_{\text{He}} c_s A_{\text{Loss}} \times 2$), with the average injection duration (0.1 s), the number of particles injected (3×10^{19} giving $\Gamma_{\text{in}} = 3 \times 10^{20}$/s), and the area for loss of He along the field (~4 cm^2), it is apparent that the local He density ($n_{\text{He}} \sim 2 \times 10^{19}$ m^{-3}) is comparable with that of

the background D ion densities. The He^+ ions and He neutrals, far from being test particles, are evidently perturbing the plasma – possibly both v_{plasma} and T_i.

6. Alternative direction of development

The requirement that the He^+ ions equilibrate with the background plasma limits the usage of this technique. An alternative diagnostic technique is to return to the standard CXRS process for measuring flows but try to accomplish it without a high-energy beam. Though providing less intense emissions, the boron ions (an intrinsic impurity arising from boronization) have the marked advantage of already having achieved equilibration with the background ions. We have evaluated the usefulness of the 494.4 nm BV line (6–7 transition) that is enhanced by B^{+5} charge exchange with locally injected D^0. Fig. 4 shows the effect on the BV line shape of puffing neutral D_2 for several frames of data. The Zeeman splitting is not resolved for the BV line indicating a high T_i (~100 eV), consistent with localization of the emission near the separatrix, and also indicating that this technique is not strongly perturbative. The use of BV CXRS emission for velocity measurements shows promise but further work is needed.

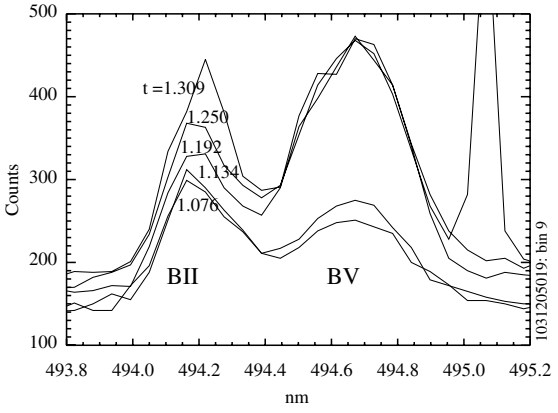

Fig. 4. Boron (BV) emissions significantly increase during the D2 puff compared to BII emission.

7. Summary

This diagnostic provides a reasonable method for obtaining relative measurements of parallel flow velocities, but only outside the separatrix with plasma temperatures <30 eV. Trends found here are consistent with those found previously for plasma flows in the SOL, but quantitative inconsistencies remain as to direction and magnitude of the flow. These are likely because of problems due to loss of high-energy ions from the field of view and the perturbative nature of the measurement. On top of these issues is an inherent inability to infer proper velocities in plasmas much hotter than 30 eV. Detailed kinetic modeling could potentially provide more accurate lineshapes when using helium as an injected neutral. Initially the BV CXRS emission (using a local gas puff) appears a better choice because the emitting ion is already in equilibrium with the background plasma.

References

[1] B. LaBombard, J. Rice, A. Hubbard, et al., Nucl. Fus. 44 (2004) 1047.
[2] N. Smick, B. LaBombard, C.S. Pitcher, Paper P1-54, these Proceedings. doi:10.1016/j.jnucmat.2004.09.035.
[3] G. Matthews, Paper R-1, these Proceedings. doi:10.1016/j.jnucmat.2004.10.075.
[4] D. Jablonski, B. LaBombard, G. McCracken, et al., J. Nucl. Mater. 241–243 (1997) 782.
[5] R.J. Fonck, D.S. Darrow, K.P. Jaehnig, Phys. Rev. A 29 (1984) 3288.
[6] A.R. Field, G. Fussmann, J.V. Hoffmann, ASDEX Team, Nucl. Fus. 32 (1992) 1191.
[7] B.L. Welch, J.L. Weaver, H.R. Griem, Phys. Plasmas 8 (2001) 1253.
[8] J. Ghosh, H. Griem, R. Elton, et al., Phys. Plasmas 11 (2004) 1033.
[9] J.L. Terry, R. Maqueda, C.S. Pitcher, et al., J. Nucl. Mater. 290 (2001) 757.
[10] A. Blom, C. Jupén, Plasma Phys. Control. Fus. 44 (2002) 1229.
[11] NRL formulary, Pub # NRL/PU/6790-94-265.
[12] G. Schmidt, Physics of High Temperature Plasmas, Academic Press, New York, 1979, pp. 387.
[13] K.L. Bell, H.B. Gilbody, J.G. Hughes et al., Culham report # CLU-R216, 1981.